Nuclear relaxation of ^{55}Mn in Ni-Mn alloys

R. L. Streever
U.S. Army Electronics Technology and Devices Laboratory, Fort Monmouth, New Jersey 07703
(Received 10 June 1974)

Nuclear relaxation times of ^{55}Mn have been studied in a series of Ni-Mn alloys containing between 1.0- and 14.4-at.% Mn using spin-echo techniques. T_1 was measured at 77 °K and in some cases at 4.2 °K as a function of external magnetic field. In the 1.0-at.% alloy T_1T increases from a value of 30 msec °K in zero field to a value of about 90 msec °K at 18 kG. At 18 kG, T_1T is found to decrease with increasing Mn concentration to a value of about 11 msec °K at 14.4-at.% Mn. Various contributions to the nuclear relaxation are evaluated both in the dilute Mn in Ni alloy and in the more concentrated alloy. In the dilute alloy, spin-wave-enhanced conduction-electron relaxation appears to be the dominant relaxation mechanism, while in the more concentrated alloys the orbital relaxation may be important.

I. INTRODUCTION

Various nuclear-magnetic-resonance (NMR) studies of nuclear-relaxation times T_1 in Ni-based alloys have been reported.[1-10] In some cases good agreement between theory and experiment has been obtained. In a number of cases, however, where the saturation method has been used to measure T_1 the results have been complicated by the appearance of a non-nuclear component in the signal recovery following saturation.[5,8,9] This non-nuclear component has been observed in studies of pure Ni metal[5] as well as in studies of the dilute Ni-based alloys.[8,9] By using annealed samples and by keeping the number of saturating pulses relatively small, the non-nuclear effects can be minimized. When this is done the resulting relaxation times for ^{61}Ni are found[5] to be in good agreement with theory, while those for ^{59}Co in Ni are found[9] to be in agreement with theory and with results of nuclear-orientation studies.[11,12]

The nuclear relaxation of ^{55}Mn in Ni is also complicated by these non-nuclear effects.[8] The present studies of the ^{55}Mn nuclear relaxation in Ni-based alloys were undertaken in an effort to clarify the nuclear relaxation in these alloys. T_1 was measured at 77 °K and in some cases at 4.2 °K as a function of external magnetic field for various Mn concentration up to 14-at.%. Some studies of T_2 and the stimulated echo decay times T_s were also made. Experimental techniques and results are discussed in Sec. II. In Sec. III various contributions to the longitudinal relaxation are discussed. In the dilute alloy, spin-wave-enhanced conduction-electron relaxation appears to be the dominant relaxation mechanism, while in the more concentrated alloys the orbital relaxation may be important.

II. EXPERIMENTAL

A. Samples

The samples were the same series of Ni-Mn alloys used in a previous study[13] which established the Mn hyperfine-field distribution. They were in powder form and contained 1.0-, 1.9-, 4.8-, 6.8-, 9.8-, and 14.4-at.% Mn. With the exception of the 1-at.% alloy no annealing of the samples was carried out since as discussed previously annealing could cause ordering in the higher-concentration alloys. In the case of the 1-at.% alloy some of the sample was annealed for approximately 2 h at 600 °C. The 1-at.% annealed sample was also prepared in an epoxy form in which the powder was dispersed in an epoxy binder which was allowed to set while the sample was in a magnetic field. The resulting samples were permanently aligned and oriented themselves freely in an applied magnetic field.

B. Measuring techniques

The spin-echo apparatus and measuring technique were described previously.[8,9] Both the saturation method as well as the stimulated echo method were used to measure T_1. Transverse relaxation times T_2 were determined from the echo decay. For the higher-concentration alloys where the NMR spectra exhibited pronounced structure the relaxation-time studies were made on the major peak of the spectral distribution (see Figs. 2 and 3 of Ref. 13).

In an effort to minimize the spurious relaxation effects which were observed previously[9] in the case of the nuclear relaxation of dilute ^{59}Co in Ni the saturation studies were made using relatively few saturating pulses (typically between 5 and 20). Under these conditions the recovery following saturation was usually exponential and nearly independent of the number of saturating pulses. The broad distribution of continuous non-nuclear resonances which were observed in the powder samples around the ^{59}Co-in-Ni frequency were not observed at the ^{55}Mn-in-Ni frequency, making the ^{55}Mn studies simpler than the ^{59}Co studies in this respect.

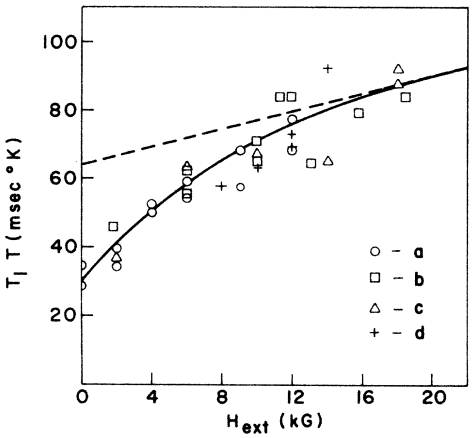

FIG. 1. Plot of T_1T versus external field H_{ext} obtained from data at 77 and 4.2 °K using various forms of the 1-at.% alloy; (a) Epoxy-annealed sample studied at 77 °K; (b) Epoxy-annealed sample studied at 4.2 °K; (c) Epoxy-unannealed sample studied at 4.2 °K; (d) unannealed powder sample studied at 77 °K. The dashed line represents an attempt to fit the data at high fields to a linear dependence (see Sec. III B).

C. Results

A plot of T_1T versus external field H_{ext} obtained from saturation method data at 4.2 and 77 °K using various forms of the 1-at.% alloy is shown in Fig. 1. Plots of T_1T versus external magnetic field obtained with the higher concentration alloys from data at 77 °K are shown in Fig. 2. A smoothed plot of the T_1T values for the 1-at.% sample is also shown in Fig. 2 for comparison. In Fig. 3 relaxation rates $(T_1T)^{-1}$ at 77 °K for both $H_{ext}=0$ and $H_{ext}=20$ kG are plotted as a function of Mn concentration.

As can be seen from Fig. 1, values of T_1T obtained using the 1-at.% annealed epoxy sample were nearly the same at 77 and 4.2 °K. With some other samples, however, this was not found to be the case. For example, the T_1T value obtained at 4.2 °K using the 1-at.% unannealed powder sample was about 34 msec °K in zero field (about the value expected from Fig. 1), but T_1 remained nearly field independent with increasing external field. Consequently, for this sample, T_1T at large values of H_{ext} was less at 4.2 °K than would be expected from the value at 77 °K. Similar behavior was observed with the 6.8-at.% unannealed powder sample. This smaller value of T_1T suggests that an additional nonintrinsic relaxation mechanism may be present in these samples.

Values of T_2 and the stimulated echo decay times T_s were also obtained with an external field of 5.6 kG. Values of T_1, T_s, and T_2 at this field are compared in Table I. Note that $T_s \approx 0.6T_1$. This ratio has been observed previously[9] in other ferromagnetic alloys. Note also that $T_1/T_2 \approx 8$. For a quadrupolar-broadened line, one expects[14] $T_1/T_2 = (I+\frac{1}{2})^2$, where I is the nuclear spin. For ^{55}Mn with $I=\frac{5}{2}$ this factor is 9, suggesting that the short value of T_2 is due to the quadrupolar broadening.

Our values of T_1T in the dilute alloy can be compared with those measured by Salamon.[3] In contrast to our result he found T_1T to be nearly field independent above 3 kG with a value of about 25 msec °K at 5 kG. This is about half our value of T_1T at the same field and somewhat less than our value of T_sT. This suggests he may have taken the T_s decay to be a measure of T_1.

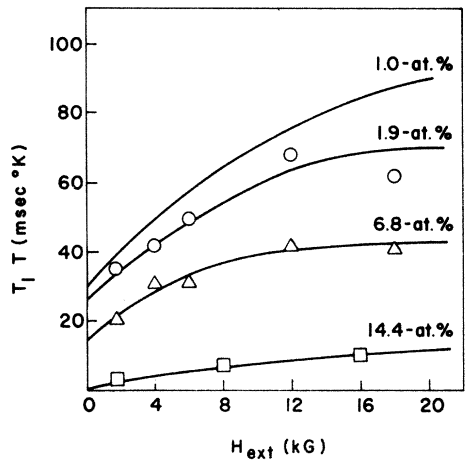

FIG. 2. Plot of T_1T versus external field obtained with the higher concentration alloys from data at 77 °K. The smoothed 1-at.% data from Fig. 1 is shown for comparison.

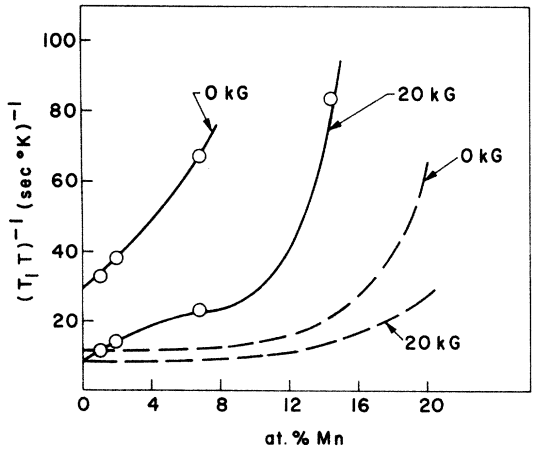

FIG. 3. Plot of experimental relaxation rates for external fields of 0 and 20 kG as a function of Mn concentration (open circles). Relaxation rates calculated from s-d mechanism (see Sec. III D) are shown for comparison (dashed lines).

TABLE I. Summary of relaxation times observed at 5.6 kG and 77 °K.

Concentration (at.%)	T_1 (msec)	T_s (msec)	T_2 (msec)
1.0	0.74	0.44	0.090
1.9	0.61	0.38	0.075
4.8	• • •	0.28	0.080
6.8	0.43	0.25	0.050
14.4	0.07	0.05	0.012

III. DISCUSSION

A. Longitudinal relaxation

The contributions to the nuclear relaxation in ferromagnetic alloys have been discussed by various authors.[1,15,16] The dominant relaxation mechanisms arise from (i) Fermi-contact interactions with s-band electrons; (ii) interactions with the orbital magnetic moments of d-band electrons; and (iii) interactions with conduction s-band electrons via spin waves. One should also consider the spin-dipolar and core-polarization relaxation mechanisms but these usually turn out to be small in comparison to the orbital relaxation contribution. Relaxation rates due to contributions (i) and (ii) can be written[16]

$$(T_1T)_s^{-1} = 2hk_B\gamma_N^2[H_{hf}(s)N_s(E_F)]^2, \quad (1)$$

$$(T_1T)_{orb}^{-1} = \tfrac{2}{5}hk_B\gamma_N^2 H_{hf}^2(\text{orb})\{[N_{d\uparrow}(E_F)]^2 + [N_{d\downarrow}(E_F)]^2\}. \quad (2)$$

The simple form of Eq. (2) occurs because equal weights of e_g and t_{2g} orbitals have been assumed. In Eq. (1), $N_s(E_F)$ is the s-band density of states at the Fermi level for one spin direction. In Eq. (2), $N_{d\uparrow}(E_F)$ and $N_{d\downarrow}(E_F)$ are, respectively, the density of states of the majority- and minority-spin d-band electrons at the Fermi level. $H_{hf}(s)$ is the 4s contact hyperfine field *per electron of an impurity* while $H_{hf}(\text{orb}) \equiv 2\mu_B\langle r^{-3}\rangle$ is the orbital hyperfine field *per unit orbital angular momentum*.

The contribution to $(T_1T)^{-1}$ from mechanism (iii) depends on the external field H_{ext} and may be written[16]

$$(T_1T)_{sd}^{-1} = A(1 + H_{ext}/B)^{-1}. \quad (3)$$

Equation (3) is valid for external fields sufficiently large that the demagnetizing and anisotropy fields can be neglected. The constant A can be written

$$A = \tfrac{1}{2}hk_B[N_s(E_F)]^2(\omega_N/S)^2(E_F/Dk_F^2)^2, \quad (4)$$

where ω_N is the resonance frequency, E_F is the Fermi energy, k_F is the Fermi momentum, and D is the spin-wave stiffness constant. B is given by

$$B = (Dk_F^2/2\mu_B)(J_{sd}S/E_F)^2. \quad (5)$$

In Eq. (5) J_{sd} is the s-d exchange integral. Equation (3) was derived for the pure host metal, but following Ref. 16 we assume it applies to the dilute alloy as well with S in Eqs. (4) and (5) taken to be the d-electron spin of the host metal.

B. Impurity relaxation times in dilute nickel-based alloys

In this section we will compare the observed relaxation times for dilute ^{55}Mn in Ni with those expected from the various mechanisms discussed in Sec. III A. To place the discussion in context we will review the corresponding situation for dilute ^{59}Co in Ni and for ^{61}Ni in pure nickel. We defer until a later section any discussion of T_1 in the more concentrated Mn-Ni alloys.

Normalized relaxation rates $R = (\gamma_N^2 T_1 T)^{-1}\times 10^7$ (sec G^2 °K^{-1}) for ^{61}Ni in pure Ni, for ^{59}Co in Ni, and for ^{55}Mn in Ni were calculated for each of the relaxation mechanisms (i)–(iii), and the results of the calculation are summarized in Table II.

In calculating the s-electron relaxation rate from Eq. (1) we have taken $2N_s(E_F) = 1.2\times 10^{11}$ states (erg atom)$^{-1}$ which is the value estimated for pure Ni by Chornik.[5] For $H_{hf}(s)$ the values given in Ref. 16 have been used, where for Ni we have interpolated to obtain a value of 1.1×10^6 G.

To evaluate the orbital relaxation rate from Eq. (2) we have taken $H_{hf}(\text{orb}) = 875$ kG for Ni, which is the value estimated by Chornik, while for Co and Mn we have used values of 510 and 350 kG, respectively.

If we assume the majority spin band is full, then $N_{d\uparrow}(E_F) = 0$. For pure Ni we take $N_{d\downarrow}(E_F) = 1.59\times 10^{12}$ states (erg atom)$^{-1}$. For the impurities (i) the values of $N_{d\downarrow}(E_F)$ can be calculated from a localized screening model.[7] Values of $\alpha_\downarrow(i)$ where

$$\alpha_\downarrow(i) = N_{d\downarrow}(E_F, i)/N_{d\downarrow}(E_F, \text{Ni})$$

are calculated in Ref. 7 to be 0.88 for Co and 0.12

TABLE II. Calculated values of the normalized relaxation rates R for various impurities in Ni and a comparison with the experimental rates at high fields; $R = (\gamma_N^2 T_1 T)^{-1}\times 10^7$ (sec G^2 °K^{-1}).

	Ni	Co in Ni	Mn in Ni
R_s	0.07	0.06	0.04
R_{orb}	7.10	1.86	0.02
R_{sd}(0 kG)	0.06	0.16	1.17
R_{sd}(20 kG)	0.05	0.12	0.94
$R_s + R_{orb} + R_{sd}$(20 kG)	7.2	2.0	1.0
R_{exp}	8.4[a]	3.9[b], 3.1[c], 1.5[d]	2.5[e]

[a] NMR, Ref. 5.
[b] NMR, Ref. 9.
[c] NMR in oriented nuclei (NMR/ON) Ref. 12.
[d] NMR in oriented nuclei (NMR/ON) Ref. 11.
[e] Value from this study at 20 kG for 1-at.%.

for Mn. Since the details of the calculation are not given in Ref. 7 we have carried out a similar calculation (see the Appendix) where we have obtained approximately the same values of $\alpha_1(i)$. We see from Table II that R_{orb} decreases rapidly in going across the series from Ni to Mn due both to a decrease in H_{hf}(orb) as well as to a decrease in $\alpha_1(i)$.

To evaluate the s-d contribution we take $S=0.3$ and use for D a value[17] of 0.89×10^{-28} erg cm^2. The Fermi energy has been taken to be 1.46×10^{-11} erg consistent with band-structure calculations[18] and k_F has been taken to be 1.41×10^8 cm^{-1} corresponding to one conduction electron per atom. This gives for ^{55}Mn in Ni a value for A of 5.1 (sec °K)$^{-1}$. Equation (4) could also be expressed in a form involving the area of the Fermi surface.[1,15] With a free-electron Fermi surface containing one conduction electron per atom a value for A of 4.3 (sec °K)$^{-1}$ would be obtained.

The parameter B is difficult to estimate as it depends on the s-d exchange integral J_{sd}. For the free atom $J_{sd}=0.15$ eV.[19] In the metal J_{sd} might be larger than this, however, and in Fe alloys a value of J_{sd} of 0.9 eV is found.[20] Using this value for J_{sd} would give a value for B of about 80 kG.

Values of R_{sd} for $H_{ext}=0$ kG and $H_{ext}=20$ kG obtained from Eq. (3) with A (for Mn) = 5.1 (sec °K)$^{-1}$ and $B=80$ kG are listed in Table II. Experimental relaxation rates at high fields are also listed in Table II where in the case of Mn in Ni the value at 20 kG obtained with the 1-at.% alloy is used. For the case of Ni and Co in Ni the s-d contribution is small in comparison with the orbital one. The total calculated relaxation rate at high fields is in fairly good agreement with the experimental one. For Mn in Ni where the s-d mechanism appears to be dominant the total calculated relaxation rate at 20 kG is about half the experimental one.

Consider now the field dependence of T_1T for Mn in Ni in more detail. At lower applied fields there may be field-dependent mechanisms other than the s-d mechanism operative so that T_1T would be less than that given by Eq. (3). At higher applied fields, however, we expect T_1T to vary linearly with applied fields as long as the s-d mechanism is dominant. The dashed line drawn in Fig. 1 would correspond to $B=50$ kG and $A=16$ (sec °K)$^{-1}$. B is the same order as the calculated value, while A is about three times the calculated value. It seems, therefore, that by assuming some enhancement of the s-d mechanism or by pulling the parameters somewhat the observed Mn-in-Ni relaxation could be explained by the s-d mechanism.

Additional support for the s-d relaxation mechanism comes from studies[10] of ^{55}Mn relaxation times in ordered Ni_3Mn where the s-d relaxation appears to be important. Since D is about the same for Ni as for Ni_3Mn, A for dilute Mn in Ni should be about 2.8 that for Mn in Ni_3Mn because of the factor S^{-2} in Eq. (4). With an A of about 2 sec °K from the Ni_3Mn studies we expect A for dilute Mn in Ni to be about 5.7 (sec °K)$^{-1}$. This is about the value calculated directly but about a factor of 3 less than the value estimated from Fig. 1.

C. Other relaxation mechanisms

In addition to the s-d relaxation mechanism already discussed there are other field-dependent relaxation mechanisms which might be important and which might explain the excess relaxation rate for zero field over that for high fields. One such mechanism would be the thermal motion of domain walls which would relax nuclei in the wings of the wall where the high-power long-time signal is thought to originate in zero field.[4] Another such mechanism would be the single magnon relaxation process discussed by Stearns.[21]

For the wall relaxation mechanism we have[1]

$$(T_1T)^{-1}_{wall}=A\nu^2[1+(2\pi\tau_c\nu)^2]^{-1}. \quad (6)$$

Here ν is the resonance frequency, τ_c is the correlation time associated with the wall motion and A depends on the magnetization, the wall width and τ_c. If A and τ_c are temperature independent the T_1T = constant relation will be satisfied.

In Table III we list for Ni and for various impurities in Ni $(T_1T)^{-1}_{excess}$ where $(T_1T)^{-1}_{excess}=(T_1T)^{-1}_{zero\,H}-(T_1T)^{-1}_{high\,H}$. Good agreement between the excess relaxation rates and the rates obtained from Eq. (6) are obtained with $A=5\times10^{-3}$ (sec °K)$^{-1}$ (MHz)$^{-2}$ and with $(2\pi\tau)^{-1}=57$ MHz. This value of τ is somewhat surprising but would be consistent with the fact that a distribution of strong non-nuclear resonances are observed[9] in Ni alloys in the frequency range around 100 MHz. These resonances may arise from some type of wall excitation. They per-

TABLE III. Comparison of $(T_1T)^{-1}_{excess}$ (the excess relaxation rate in zero field over that at high field) with the values of $(T_1T)^{-1}_{wall}$ calculated from Eq. (6).

Nucleus	ν (MHz)	$(T_1T)^{-1}_{excess}$ (sec °K)$^{-1}$	$(T_1T)^{-1}_{wall}$ (sec °K)$^{-1}$	R_{excess}
Ni^{61}	28	4[a]	3	7.0
Ru^{101}	48	5[b]	7	30
Cu^{63}	56	9[c]	8	1.8
Co^{59}	120	29[d]	14	7.4
Pt^{195}	310	20[e]	16	6.0
Mn^{55}	343	22[f]	16	5.1

[a]References 4 and 5.
[b]Reference 7.
[c]Reference 4.
[d]Reference 9.
[e]Reference 6.
[f]This work based on high-field value at 20 kG.

sist up to relatively high values of the applied field and may be associated with pinned domain walls.

In the case of Mn in Ni and to some extent Co in Ni and Ni where the calculated intrinsic relaxation rates are less than the experimental rates, the wall relaxation may be important even at high fields. In fact, if we add about one-fourth of the normalized excess relaxation rate to the total calculated intrinsic relaxation rates given in Table II we obtain relaxation rates in good agreement with the experimental relaxation rates at 20 kG.

Wall relaxation effects might also explain the departure from the T_1T = constant relation observed in the unannealed powder samples.

D. Concentration dependence of T_1

If the s-d relaxation mechanism were the dominant one for Mn in Ni then one would expect the relaxation to be dependent on concentration because of the concentration dependence of the various factors in Eq. (4). The concentration dependence of the spin-wave parameter D can be related to that of the Curie temperature by the approximate relation[22]

$$D \propto T_C/(\bar{S}+1). \tag{7}$$

In (7), T_C is the Curie temperature and $\bar{S}$ is the average spin of the alloy. With increasing of Mn concentration, T_C is known to decrease which should result in a decrease in D and an increase in the s-d relaxation rate. Assuming that in Eqs. (4) and (5), $S=\bar{S}$ and that only $\bar{S}$, D, and ω_N depend on concentration, we have calculated the concentration dependence of the parameters A and B from the experimental values[23] of T_C and $\bar{S}$ at each concentration.

We have then used Eq. (3) to calculate $(T_1T)^{-1}_{sd}$ at both zero field and at 20 kG. In the dilute alloy B has been taken to be 50 kG. A has been taken to be 12 (sec °K)$^{-1}$ in order that the calculated and experimental relaxation rates agree in the dilute alloy. The result of the calculation is shown in Fig. 3. Although there is some similarity between experimental and calculated relaxation rates, the experimental rates at both zero field and 20 kG increase more rapidly with Mn concentration than do the calculated ones. Actually, a simple relation like (7) used to calculate D would not be expected to hold well at the higher Mn concentrations where antiferromagnetic exchange interactions between Mn atoms become important.

Also note that the high-field relaxation rate follows to some extent the zero-field rate suggesting that the pinned wall relaxation might be important. The wall relaxation rate might be expected to increase with increasing Mn concentration if the pinning were due to Mn atoms.

The single-magnon relaxation discussed by Stearns would also be expected to increase with Mn concentration due to a decrease in D. Also at the higher Mn concentrations some Mn spins would see relatively small effective exchange fields due to the competing ferromagnetic and antiferromagnetic interactions.

E. Orbital relaxation at higher concentrations

As was discussed in Sec. III B the density of states for Mn in the dilute Ni-based alloy as calculated on a localized model turns out to be small. Physically, this is due to the fact that the whole spin-up band including any Mn localized level should lie below the Fermi level, while in the spin-down band the Mn localized level should lie well above E_F.[24] In the more concentrated alloy, however, the situation should be quite different. The nearest-neighbor Mn-Mn interaction is antiferromagnetic. Consequently, as was discussed in Ref. 13, at higher Mn concentrations when a given Mn atom has about three or more nearest neighbors the central Mn atom becomes antiferromagnetically aligned with respect to the neighbor moments. This can explain the decrease in magnetization at the higher Mn concentrations above 10%. From the band-structure point of view the decrease in the magnetic moment has to be attributed to an extension of the spin-up band across the Fermi level as has been discussed recently by Hasegawa and Kanamori[25] who calculate the band structure using the coherent potential approximation.

The potentials acting on the localized levels are spin dependent,[26] and on a more localized picture we can think of the Mn spin-up localized level as being pushed across the Fermi level with increasing Mn concentration due to the antiferromagnetic exchange interaction with neighboring Mn atoms. We might expect the density of states for the Mn to increase rapidly at around 10-at.% Mn as the localized spin-up level crosses the Fermi level with a corresponding increase in the orbital relaxation rate.

Assuming that

$$(T_1T)^{-1}_{\text{orb}} = (T_1T)^{-1}_{\text{exp}} - (T_1T)^{-1}_{sd}$$

and using the 20-kG data from Fig. 3 we have calculated $N_{d\uparrow}(E_F, \text{Mn})$ from Eq. (2) as a function of concentration assuming $N_{d\downarrow}(E_F, \text{Mn}) = 0$. Values of $\alpha_\uparrow$(Mn), which is the value of $N_{d\uparrow}(E_F, \text{Mn})$ relative to the density of states in the spin-down band of pure Ni at E_F, are shown in Fig. 4. The rapid rise in α around 10-at.% Mn would be consistent with the preceding discussion. The values of $\alpha_\uparrow$(Mn) shown in Fig. 4 may not be unreasonably large if we consider that the localized level is relatively narrow. For the fully occupied localized level $N_{d\uparrow}(E_F) = 5/\pi\Delta$ when the localized level sits on the

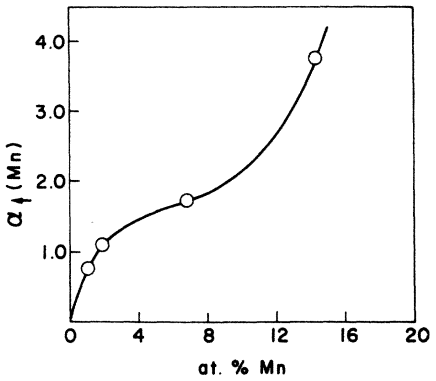

FIG. 4. Values of $\alpha_\uparrow$(Mn) the relative density of states at the Mn atom in the spin-up band as a function of Mn concentration calculated as discussed in text from Eq. (2).

Fermi level. Here 2Δ is the width of the localized level.[7] Using a value[27] for Δ of 0.14 eV we get $N_d(E_F, \text{Mn}) = 11$ states (eV atom)$^{-1}$ or $7\times10^{+12}$ states (erg atom)$^{-1}$. This is about four times the pure-Ni density of states at E_F.

The average density of states per atom at E_F can also be calculated as a function of Mn concentration from the values of $\alpha_\uparrow$(Mn) if one assumes the Ni density of states per atom is constant. At 14-at.% Mn the average density of states at E_F relative to pure Ni turns out to be 1.35. This compares with a corresponding change in specific-heat capacity at 20-at.% Mn and 25-at.% Mn of 1.27 and 1.32, respectively.[28]

IV. CONCLUSION

For Ni metal and for Co in Ni the s-d relaxation mechanism is relatively small in comparison with the orbital one. For dilute Mn in Ni, however, where the orbital relaxation should be small, the s-d relaxation mechanism appears to provide the dominant intrinsic contribution to the nuclear relaxation. The calculated Mn in Ni relaxation rate from the s-d mechanism is, however, about a factor of 2 smaller than the observed relaxation rate. The difference between the calculated and observed relaxation rates may be due to the effects of pinned domain walls which may persist up to relatively high values of the applied magnetic field.

The marked increase in Mn relaxation rate observed with increasing Mn concentration appears to be due in part to the increase in s-d relaxation and in part to the increase in orbital relaxation which may become important at the higher Mn concentrations.

TABLE IV. Values of $\alpha_\downarrow(i)$, the relative density of states at the impurity calculated from Eq. (8), for the $d\epsilon$ and $d\gamma$ subbands. Values of the impurity potential $V_\downarrow(i)$ are also listed.

Impurity (i)	$V_\downarrow(i)$[a] (eV)	$\alpha_\downarrow(i)$[b] $d\epsilon$ band	$\alpha_\downarrow(i)$[b] $d\gamma$ band	$\overline{\alpha_\downarrow(i)}$[c]	$\alpha_\downarrow(i)$[d]
Co	.54	0.61	1.2	0.85	0.88
Fe	1.01	0.30	0.39	0.34	0.35
Mn	1.90	0.10	0.09	0.10	0.12

[a]From Ref. 29
[b]Calculated from Eq. (8).
[c]Weighted average.
[d]Values from Ref. 7.

ACKNOWLEDGMENT

The author wishes to thank P. J. Caplan for his assistance during the experimental stages of the work.

APPENDIX

In this section we calculate the density of states at the impurity at the Fermi level for the minority spin band of the dilute alloy. From Ref. 16, we have

$$N_{d\downarrow}(E_F, i) = \frac{N_{d\downarrow}(E_F, \text{Ni})}{\left[1 - \frac{1}{5} V_\downarrow(i) F_\downarrow(E_F)\right]^2 + \left[\frac{1}{5}\pi V_\downarrow(i) N_{d\downarrow}(E_F, \text{Ni})\right]^2}. \quad (8)$$

Here $N_{d\downarrow}(E_F, i)$ is the total density of states at the impurity at the Fermi level, $N_{d\downarrow}(E_F, \text{Ni})$ is the corresponding quantity for the pure host metal, $F_\downarrow(E)$ is the Hilbert transform of $N_{d\downarrow}(E_F, \text{Ni})$, and $V_\downarrow(i)$ is the impurity potential in the minority spin band. $N_{d\downarrow}(E_F, \text{Ni})$ has about the same value in the $d\epsilon$ and $d\gamma$ subbands so we use an average value of 2.54 states (ev atom)$^{-1}$ consistent with the value used previously. The value of $F_\downarrow(E_F)$ is sensitive to the details of the band structure, however.[29] From Figs. 1 and 2 of Ref. 29 we obtain for $F_\downarrow(E_F)/N_{d\downarrow}(E_F, \text{Ni})$ a value of 0.2 for the $d\epsilon$ bands and 2.5 for the $d\gamma$ bands. Values of $\alpha_\downarrow(i)$ calculated for the two bands are shown in Table IV where as defined in Sec. III,

$$\alpha_\downarrow(i) = N_{d\downarrow}(E_F, i)/N_{d\downarrow}(E_F, \text{Ni}).$$

The values of $V_\downarrow(i)$ are taken from Ref. 29. The weighted average of $\alpha_\downarrow(i)$ over the two bands is in approximate agreement with the values given in Ref. 7.

[1]M. Weger, Phys. Rev. 128, 1505 (1962).
[2]R. L. Streever, Phys. Rev. 134, A 1612 (1964).
[3]M. B. Salamon, J. Phys. Soc. Jap. 21, 2746 (1966).
[4]M. H. Bancroft, Phys. Rev. B 2, 182 (1970).
[5]B. Chornik, Phys. Rev. B 4, 681 (1971).
[6]R. L. Streever and P. J. Caplan, in *Proceedings of the Seventeeth Annual Conference on Magnetic Materials*, 1971, edited by C. D. Graham, Jr. and J. J. Rhyne

(A.I.P., New York, 1972).
[7]J. Durand, F. Gautier and C. Robert, Solid State Commun. 11, 1213 (1972).
[8]R. L. Streever and P. J. Caplan, Phys. Rev. B 7, 4052 (1973).
[9]R. L. Streever and P. J. Caplan, Phys. Rev. B 8, 3241 (1973).
[10]R. L. Streever, in *Proceedings of the Nineteenth Annual Conference on Magnetic Materials*, 1973, edited by C. D. Graham Jr. and J. J. Rhyne (A.I.P., New York, 1974).
[11]D. Spanjaard, R. A. Fox, I. R. Williams, and N. J. Stone in *Hyperfine Interactions in Excited Nuclei*, edited by G. Goldring and R. Kalish (Gordon and Breach, New York, 1971).
[12]F. Bacon, J. A. Barclay, W. D. Brewer, D. A. Shirley and J. E. Templeton, Phys. Rev. B 5, 2397 (1972).
[13]R. L. Streever, Phys. Rev. 173, 591 (1968).
[14]R. E. Walstedt, Phys. Rev. Lett. 19, 146 (1967); 19 816 (1967).
[15]T. Moriya, J. Phys. Soc. Jap. 19, 681 (1964).
[16]M. Kontani, T. Hioki, and Y. Masuda, J. Phys. Soc. Jap. 32, 416 (1972).
[17]H. A. Mook, J. W. Lynn, and R. M. Nicklow, Phys. Rev. Lett. 30, 556 (1973).
[18]J. Callaway and C. S. Wang, Phys. Rev. B 7, 1096 (1973).
[19]W. Marshall, Phys. Rev. 110, 1280 (1958).
[20]M. B. Stearns, Phys. Rev. B 4, 4081 (1971).
[21]M. B. Stearns, Phys. Rev. 187, 648 (1969).
[22]M. Hatherly *et al.*, Proc. Phys. Soc. Lond. 84, 55 (1964).
[23]S. Kaya and A. Kussmann, Z. Physik 72, 293 (1931).
[24]J. Freidel, *Proceedings of the Varenna School*, 1966, edited by W. Marshall (Academic, New York, 1967).
[25]H. Hasegawa and J. Kanamori, J. Phys. Soc. Jap. 33, 1599 (1972).
[26]I. A. Campbell and A. A. Gomes, Proc. Phys. Soc. Lond. 91, 319 (1967).
[27]R. Caplain, R. Caudron, and P. Costa, C. R. Acad. Sci. (Paris) 276, 741 (1973).
[28]W. Proctor, R. G. Scurlock, and E. M. Wray, Proc. Phys. Soc. Lond. 90, 697 (1967).
[29]H. Hayakawa, Prog. Theor. Phys. 37, 213 (1967).